Signal Processing Techniques for On-Line Partial Discharge Detection and Classification

Alex Aranburu[*], *Jon Olaizola*[*], *Maitane Barrenechea*[*], *Patrick Mulroy*[†], *Aritz Hurtado*[†] *and Ian Gilbert*[†]

[*]Mondragon Unibertsitatea
[†]Ormazabal Corporate Technology, A.I.E.

ABSTRACT

Partial discharge (PD) detection plays a fundamental role in monitoring the health of medium voltage (MV) systems. This paper presents a method for PD detection and source recognition in MV sub-stations based on a combination of signal processing techniques. Firstly, PD detection and signal conditioning is carried out. Then, PDs of different sources are separated and finally classified by means of the extension set theory. The obtained results show a classification effectiveness of 100% on single source PDs and an effectiveness of 72.5% in multisource PDs, where PDs from many sources are captured in the same data set.

Index Terms— partial discharge, PD, pattern recognition, classification, extension set theory.

1. INTRODUCTION

A partial discharge (PD) is a localized electrical discharge which manifests itself as a high frequency, short duration signal that may be propagated through the cables and equipment of an electrical network. Their detection and source identification may lead to medium voltage (MV) network health monitoring, providing useful information to network owners for operation and maintenance programming and investments.

Traditionally one of the most complete representation methods of PD data has been the so-called phase-resolved partial discharge (PRPD) patterns. Here a discharge quantity (such as the magnitude or the number of discharges) is plotted against the ac phase. The success of such plots to represent different types of PD can be attributed to the fact that they can be related to parameters physically describing the PD process [1]. One of the major drawbacks of phase plots is that they have limited use in online measurements where the data may be corrupted by pulse-shaped interference or multiple sources being simultaneously present.

In the recent years, new PD detection and identification methods based on artificial intelligence techniques have been developed. For example, fuzzy clustering [2] and neural networks (NN) [3] have been extensively used in PD recognition. The fuzzy approaches require human expertise and have been successfully applied to this field. However, there are difficulties in acquiring knowledge and in maintaining the database. The main advantage of the NN is that they can directly acquire experience from the training data. A great limitation of the NN approach is the inability to use a linguistically descriptive output, because it is difficult to understand the content of a network.

Recently, new PD detection and classification techniques have been designed. An approach based on the radial basis function (RBF) NN for identifying insulation defects of high-voltage electrical apparatus arising from PD has been developed [4]. Although the operation speed of neural networks allows real time PD classification, its training process can be often slowly depending on the amount of different patterns that are available.

The following chapters describe a new method to successfully detect and classify PD sources, overcoming the difficulties of the aforementioned techniques. In order to do so, a combination of PD pattern recognition, source separation and pattern classification methods have been applied. A general block diagram of the proposed system is shown in Figure 1.

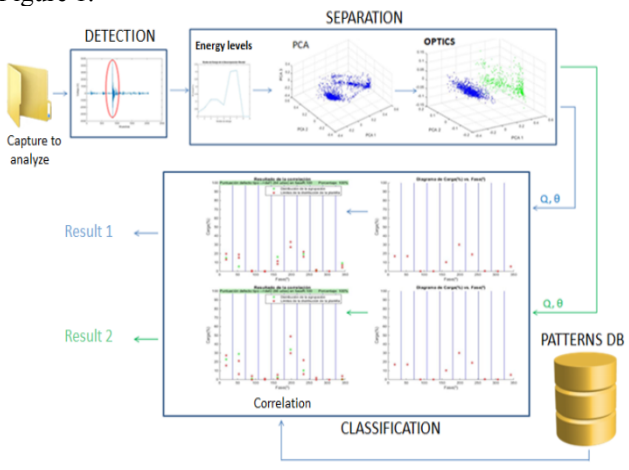

Fig. 1. General block diagram

2. PD DETECTION AND CONDITIONING

Partial discharges in medium voltage (MV) systems have been detected with a single two-output sensor: one of the outputs gives the high-frequency signal present in the MV system and contains the PD signals generated in the MV

978-0-9928-6265-7/16/$31.00 ©2016 IEEE

system. The other low-frequency output represents the attenuated power frequency energy carrying sinusoid which is used for PD phase estimation.
Unfortunately, the medium-voltage system does not operate in an ideal environment. That is why many artifacts may appear in the high-frequency components signal such as white noise, oscillations, impulsive noise, etc. These artifacts can modify the waveform of partial discharge signals or they can even be detected as if they were PDs. To avoid this, signal processing techniques are applied to condition the signal before its analysis and classification.

2.1. PD denoising

Thanks to some denoising methods, the resulting high-frequency signal becomes a much smoother signal, where PDs can then be detected easily. In addition, other measures are also applied to each detected peak so that falsely detected PDs are rejected. As a result, white noise, impulsive noise, reflections, and both oscillations produced by reflections and very high amplitude PDs are discarded. All this leads to a correct detection stage, which is extremely important for subsequent stages.
Firstly, discrete wavelet transform (DWT) can be used to successfully eliminate white noise [5]. The effects of this method can be seen in Figure 2. Although PD amplitude is decreased, noise is considerably reduced.

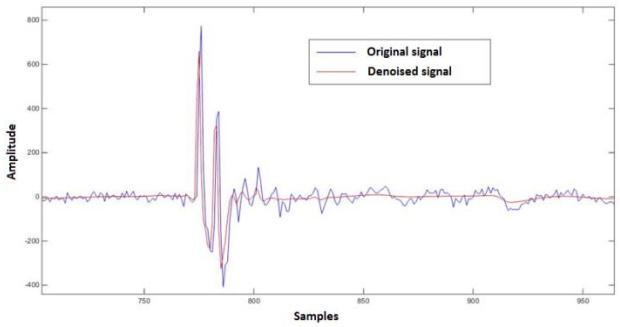

Fig. 2. Discrete wavelet transform (DWT) denoising

This denoising is achieved by means of a 3 level DWT, from which detailed and approximate coefficients are obtained. For this particular application, the mother wavelet 'Symlet 9' has been chosen, which has been shown to be the most suitable for PD signal conditioning [6]. After the decomposition, the most meaningful coefficients are discriminated with hard thresholding. Finally, inverse DWT is computed to build the denoised signal.
Further peak detection parameters are also employed in order to discard impulsive noise and some oscillations from the signal envelope. Prominence is calculated as shown in (1) and compared to a minimum threshold. This removes small impulsive noise by only selecting the main peaks in the envelope. The prominence of a peak represents how much the peak stands out considering its height and its position relative to other peaks. For each peak, the valleys between it and a higher peak (or the end of the signal if there are not higher peaks) are found at both sides. Afterwards, the minimum valley is estimated at each side and the reference level is set as the highest valley between the two. Finally, the peak prominence is specified by the height of the peak above this reference level. While PDs are commonly the main or prominent peaks, impulsive noise detected as peaks will be discarded because it will not exceed minimum peak prominence percentage.

$$prominence(\%) = \frac{peak\ prominence}{peak\ amplitude} \cdot 100. \quad (1)$$

When reflections in the MV system produce oscillating signals, multiple uniform peaks are generated very close to one another and translates to a single, very wide peak in the signal envelope. If a maximum peak width is established (around 312 ns), as illustrated in Figure 3, these kinds of oscillations can be discarded.

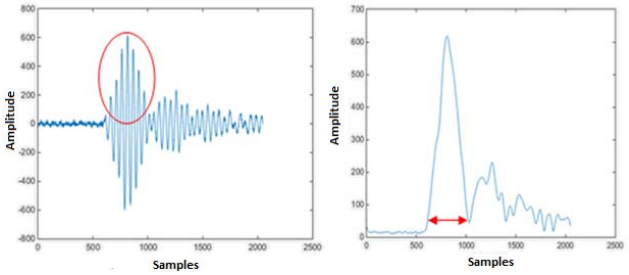

Fig. 3. Rejection of high frequency oscillations caused by reflections with max. peak width

Other types of oscillations have also been found, produced by very high amplitude PDs. These oscillations might affect PD detection in two different ways. Oscillations may modify the waveform of successive PDs and/or big oscillations may also be detected as PD peaks. Both effects can be seen in Figure 4.

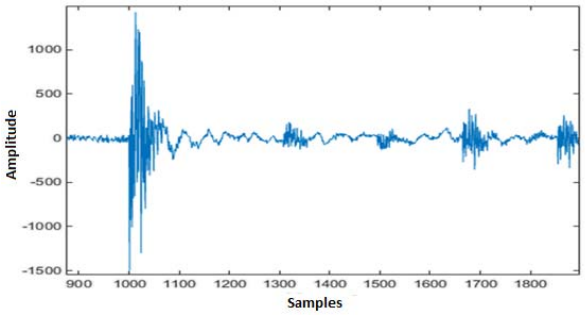

Fig. 4. Rejection of low frequency oscillations caused by very high amplitude PDs with threshold

To solve this, a threshold has been established that detects these kinds of very high amplitude peaks. When a peak exceeds this threshold, only that peak is taken into account in that window (2048 samples), whereas the rest of the peaks are discarded. Hence, although the number of detected peaks decreases, this filter does not change the results significantly.
Lastly, a tunable notch filter has been implemented to remove other RF interference signals. First of all, the FFT (Fast Fourier Transform) and the normalized frequency spectrum of the window are obtained. In the low frequency range (below 10 MHz), sharp dominant frequencies are detected and the centre frequency of the notch filter is tuned according to these dominant frequencies in order to eliminate them. Figure 5 represents the original signal with its

frequency spectrum and Figure 6 illustrates the filtered signal, free of oscillations with its frequency spectrum, free of dominant frequencies.

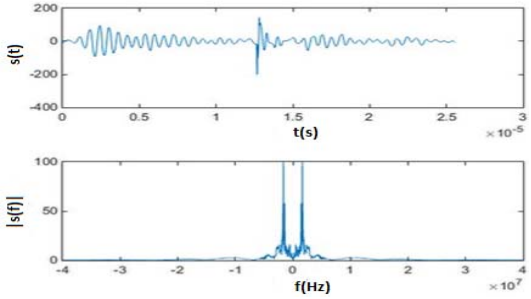

Fig. 5. Original signal with its frequency spectrum

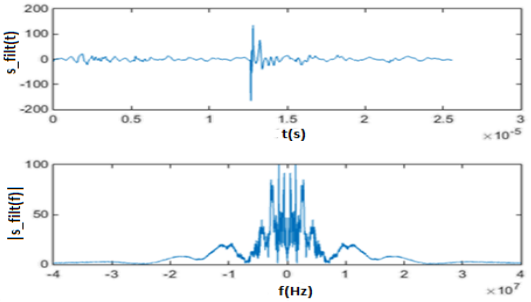

Fig. 6. Filtered signal, free of oscillations; with its frequency spectrum,

2.2. PD detection

After a PD has been detected, it is necessary to determine its start and end point. With these reference points it is then possible to isolate the PD from the rest of the signal. In order to find those points, the Energy Criterion (EC) method is employed [7]. Each sample in the EC signal is defined as:

$$EC(n) = \sum_{i=1}^{n} x(i)^2 - \frac{n}{N} \cdot \sum_{i=1}^{N} x(i)^2, \quad (2)$$

where n ranges from 1 to N and N is the number of samples in a window (2048 in this case). With this EC signal, big amplitude changes produced in the original signal can be detected. Using this information, the starting point of the PD is defined as the minimum point of the EC signal, whereas the end is defined as the point where the gradient of the EC signal starts to be negative and continuous (Figure 7).

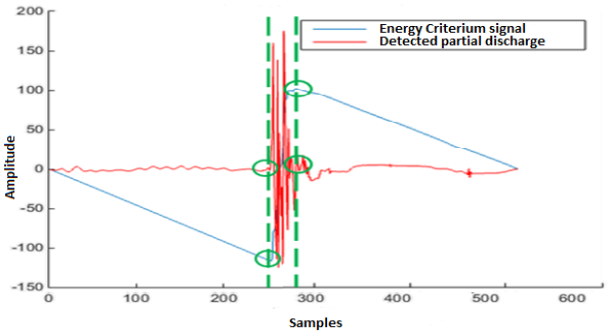

Fig. 7. PD start and end point estimation with EC signal

3. DEFECT PATTERN GENERATION

Once all the PDs have been detected and isolated, the generation of a representative model is needed so that a successful PD classification can take place. The classification stage will correlate the representative model of an analyzed capture with the patterns of all PD types. It is for this reason that these patterns need to be generated beforehand. Every single pattern is created taking into account the representative models of all captures of the same PD or defect type. These model PDs are generated in a controlled laboratory and stored in a PD database.

In this case, an Average Charge (%) versus Phase Window (º) (ACPW) diagram is used as the aforementioned representative model. The ACPW diagram is computed for each capture, where the 50 Hz frequency power signal is used for phase estimation of PDs detected in the high-frequency signal. The phase is divided in ten windows of 36º and the percentage of the total charge for each window is computed. An example of this diagram has been illustrated in Figure 8.

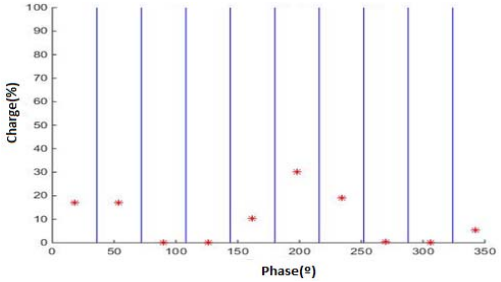

Fig. 8. ACPW diagram of a single capture

By combining the ACPW diagrams of various PD signals obtained from the same type of defect, the maximum and minimum average charge for each phase window is computed. These will represent the ranges of the pattern of that defect type, as it can be seen in Figure 9.

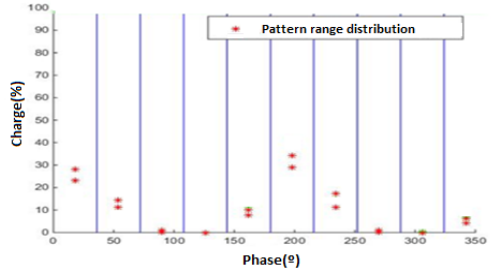

Fig. 9. ACPW diagram of a pattern

4 DEFECT SEPARATION

It is possible that more than one defect is present in the same MV system. Thus, many PD types could be manifested in the same capture. To separate them correctly, Wavelet Energy Levels are computed for each detected PD. Commonly, energy levels are estimated from standard DWT. However, a static bandwidth is set with this transform (each level has the half of the bandwidth of the previous level). In consequence, it has been found that in some cases two different PD types may have very similar wavelet energy levels, although the PD waveform and frequency

spectrum is different. Figure 10 shows two PD types and Figure 11 illustrates their respective energy levels. As we can see from this example, even if the PDs are completely different, their associated wavelet energy levels are almost identical. This may lead to errors in the PD separation process.

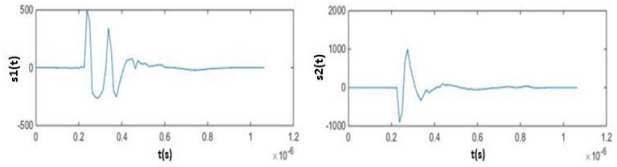

Fig. 10. PDs generated by defects 1 and 2.

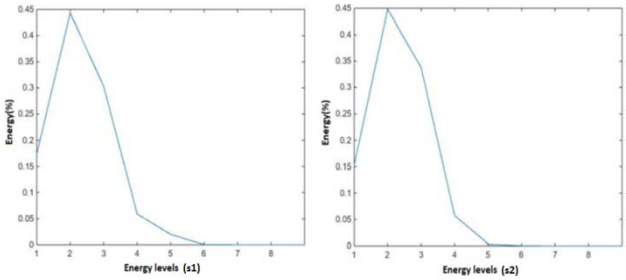

Fig. 11. Energy levels of the PDs generated by defects 1 and 2.

As it has been proved that energy levels with dynamic or flexible bandwidth improve results and increase their variability, the Laguerre Transform [8] has been employed to define 8 energy levels (between 0-40 MHz), each with 5 MHz bandwidth. As a result, energy levels become more variable and this enables the algorithm to separate defect types easier. Thanks to this transform, the frequency spectrum of every PD is mapped conveniently with (3) and (4) where w_c is the desired center frequency.

$$\theta(w) = w + 2 \cdot \arctan\left(\frac{b \cdot \sin(w)}{1 - b \cdot \cos(w)}\right) \quad -1 < b < 1. \ (3)$$

$$b(w_c) = \tan\left(\frac{\pi}{4} - \frac{w_c}{2}\right). \ (4)$$

Nevertheless, the Laguerre Transform is not energy conserving. Hence, in order to obtain a new energy conserving spectrum $\theta(w)_{esc.}$, a scaling step is required, which is carried out with (5) and (6).

$$\theta(w)_{esc.} = \sqrt{\theta(w)'} \cdot \theta(w). \ (5)$$

$$\sqrt{\theta(w)'} = \frac{1-b^2}{1-2 \cdot b * \cos(w)+b^2} = \frac{\sqrt{1-b^2}}{1-b \cdot e^{-j \cdot w}}. \ (6)$$

To conclude, energy levels are calculated with a standard DWT of the modified signal. Figure 12 illustrates the new energy levels of the previous two PD types after the application of the Laguerre Transform. As shown in this figure, the wavelet energy levels of both PD types are different and can now be successfully separated.

Once the energy levels of all PDs in a capture have been computed, the most representative energy levels have to be selected (the ones with highest variability). This dimensionality reduction is achieved by means of the principal component analysis (PCA) algorithm [9]. By selecting the three most significant energy levels, the PDs can be mapped into a 3D space and, therefore, different PD types can be visually separated as represented in Figure 13.

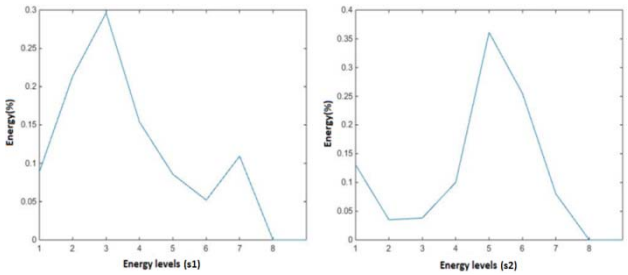

Fig. 12. Energy levels of the PDs generated by defects 1 and 2 after the Laguerre Transform

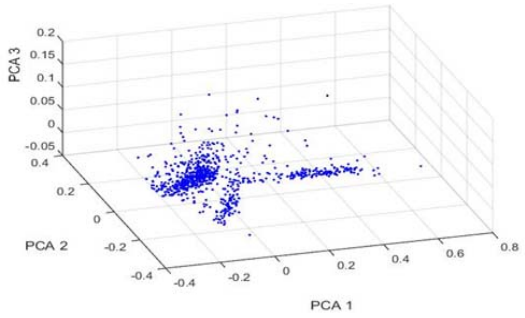

Fig. 13. 3D PCA space of a three PD type capture

Although different PD groups can be visually distinguished, this process needs to be automated by means of a clustering algorithm. This is achieved with the OPTICS (Ordering Points To Identify the Clustering Structure) algorithm [10]. For that, a reachability plot is used, where each cluster or group is represented as a valley, as illustrated in Figure 14. The results of the PD clustering process are shown in Figure 15.

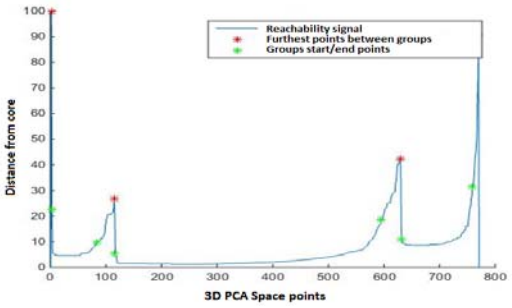

Fig. 14. Reachability plot of the previous 3D PCA Space

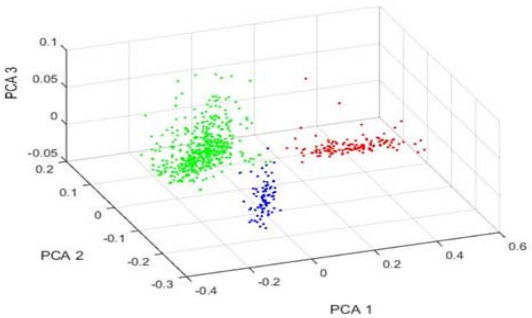

Fig. 15. PD type separation by OPTICS in the 3D PCA Space

5. PD CLASSIFICATION

Once the different PD clusters have been defined, each PD type has to be identified. This classification process is carried out by means of the extension set theory [11]. In order to do this, each PD cluster's ACPW diagram (*i*) is correlated with the pattern diagrams saved in the database (*j*) [12]. The correlation result K_{ij} (7-9) is estimated with points *f* and *g* defined from points *a* (range minimum) and *b* (range maximum), where $X_0 = [a,b]$ and X= *[f,g]* and $f=0,8a$ and $g=1.2b$.

$$K_{ij}(x) = \begin{cases} \frac{-2 \cdot p(x,X_0)}{b-a}, & x \in X_0 \\ \frac{p(x,X_0)}{p(x,X)-p(x,X_0)}, & x \overline{\in} X_0 \end{cases} . (7)$$

$$p(x,X_0) = \left| x - \frac{a+b}{2} \right| - \frac{b-a}{2}. (8)$$

$$p(x,X) = \left| x - \frac{f+g}{2} \right| - \frac{g-f}{2}. (9)$$

6. RESULTS

Satisfactory results have been achieved with different voltages (10 kV, 20 kV and 30 kV) and in various environments. Up to six PD type signals generated on a MV distribution network (sourced from defective installation, such as a missing busbar end-plug or disconnected earth braid) have been employed. The algorithm has been tested in a triphasic environment, although it can also be used in monophasic systems.

Regarding the working voltage of the MV system, it has been observed that the algorithm works better when high voltages are employed, as the number of PDs increases in these cases. Table 1 represents the effectiveness percentage of the algorithm.

	Effectiveness percentage
Single PD type	100%
Multiple PD types	72.5%

Table 1. Final results statistics

The algorithm has classified successfully single PD type captures in 100% of the cases. However, the effectiveness with captures having multiple PD types has been of 72.5%. The lower effectiveness of the algorithm in multi-defect scenarios is due to a wide variation in PD repetition rates of the different PD types. This PD number imbalance hinders the PD clustering process by identifying a single PD cluster instead of two. This leads to just a single defect type being identified correctly. This outcome has been considered as an erroneous output of the algorithm when calculating the effectiveness ratio in Table 1. However, it is possible to correct the first detected defect and then run the algorithm again. In this case, the second defect (which generates a small number of PDs) can be successfully identified. This way, effectiveness ratio of the algorithm would increase up to 88% in the identification of multiple defects.

7. CONCLUSIONS

This paper has presented an innovative defect detection and classification system. Unlike other algorithms found in the literature, the proposed PD detection and classification system has been tested in a real environment where a variety of artifacts are present. The algorithm requires minimum training (just the generation of the defect patterns) and has been proven to work correctly in both monophasic and triphasic environments. It provides a good solution to on-line PD detection and classification in MV systems.

ACKNOWLEDGMENT

This work was supported by the Spanish Government (Ministerio de Economía y Competitividad) under the project RTC-2014-1713-3 OPTIMUS.

REFERENCES

[1] C. Heitz, "A generalized model for partial discharge processes based on a stochastic process approach", Journal of Physics D: Applied Physics 32(9), pp. 1012–1023, 1999.

[2] Li, X., "Fuzzy self-organizing maps for detection of partial discharge signals," In Proceedings of IEEE/ASME international conference on advanced intelligent mechatronics, pp. 1683–1688, 2009.

[3] Chen, H. C., Gu, F. C., & Wang, M. H., "A novel extension neural network based partial discharge pattern recognition method for high-voltage power apparatus", Expert Systems with Applications, 39(3), pp. 3423-3431, 2012.

[4] Chang, W. Y. "Partial Discharge Pattern Recognition of Cast Resin Current Transformers Using Radial Basis Function Neural Network", Journal of Electrical Engineering & Technology, 9(1), pp. 293-300, 2014.

[5] Pradhan, A. K., "Analysis of partial discharge signals using digital signal processing techniques", National Institute of Technology Roukela, 2012.

[6] Hao, L et al., "Discrimination of Multiple PD Sources Using Wavelet", s.1.. IEEE, 2011

[7] Wagenaars, P., "Integration of Online Partial Discharge Monitoring and Defect Location in Medium-Voltage Cable Networks", Eindhoven University of Technology, pp. 74-75, 2010.

[8] Evangelista, G., "Flexible Wavelets for Music Signal Processing", Journal of New Music Research, 30(1), pp. 13–22, 2001.

[9] Moore, B., "Principal component analysis in linear systems: Controllability, observability and model reduction", Automatic Control, IEEE Transactions on, 26(1), 2003.

[10] Ankerst, M., Breunig, M. M., Kriegel, H.-P. & Sander, J., "OPTICS: Ordering Points To Identify the Clustering Structure", University of Munich, 2004.

[11] Ho, C.-Y., Wang , M.-H., "Application of Extension Theory to PD Pattern Recognition in High-Voltage Current Transformers", 2005.

[12] Gu, F.-C., M.-H. Wang & Chen, H.-C., "A novel extension neural network based partial discharge pattern recognition method for high-voltage power aparatus", ScienceDirect, 2012.